Single-User MIMO ML Successive Interference Canceling Receiver with HARQ-IR Protocol

Elena Lukashova, Florian Kaltenberger, Raymond Knopp
EURECOM
Campus SophiaTech, 450 Route des Chappes,
06410 Biot, France
Email: (elena.lukashova@eurecom.fr)

***Abstract*—Incremental Redundancy Hybrid Automatic Repeat Request (HARQ-IR) retransmission protocol was developed to reduce the transmission errors over fading channels through multiple retransmissions. In this paper, we implement HARQ-IR for Single User MIMO systems with Successive Interference Canceling (SIC) receiver. We perform the throughput and reliability analysis for the MIMO system with Closed Loop Spatial Multiplexing (TM4) with two codewords (CW) and compare the results for SIC and Parallel Interference Aware (PIA) receiver. Our SIC receiver benefits from the log-likelihood ratios combining for the second transport block, accessed through the multi-round SIC procedure a posteriori to all the previous rounds once the first CW has been decoded, while PIA receiver treats both CWs in the same manner. The SIC receiver achieves higher throughput in frequency selective environment, receiving most of the gain in the first two retransmission rounds. For both receivers, the first transport block enjoys huge performance improvement in the low SNR regime thanks to HARQ at the price of spectral efficiency degradation due to reuse of the space-frequency resources. We also investigate the optimal retransmission scheme for TM4 in the scenarios with one successfully decoded CW, while another one is in error.**

I. Introduction

LTE has been designed to allow maximum flexibility in exploiting the benefits of MIMO channels. The so called transmission modes (TM) range from transmit diversity, over beamforming to spatial multiplexing. At the same time, Hybrid Automatic Repeat Request (HARQ) retransmission protocols were developed to reduce the transmission errors over fading channels through multiple retransmissions. If the CW is successfully decoded, the UE sends an acknowledgment message (ACK) on the one of the uplink channels and the eNodeB proceeds to the transmission of the next data packet. In the opposite case, the UE sends a non-acknowledgment message (NACK) and the eNodeB retransmits the package. At the UE side, the log-likelihood ratios (LLR) of the corresponding bits will be added up and the new decoding attempt will be performed.

HARQ protocol has two options: Chase Combining (CC) and Incremental Redundancy (IR) [1]. HARQ-CC can be thought of as a repetition code: upon reception of the NACK message, the eNodeB resends exactly the same copy of previously transmitted message. Thus, there is no coding gain provided by this method. On contrary, using more complex IR type of the protocol, the eNodeB sends a different redundancy version (RV) of the message at each retransmission round. The RV is generated from the different fractions of the systematic and parity check bits, delivering coding gain with every new retransmission. HARQ-IR, that is in focus of this paper, is shown to outperform the HARQ-CC in the majority of the scenarios.

The fundamental analysis of the HARQ protocols in Gaussian collision channel was done by Caire and Tuninetti [2], where the authors derived the closed-form expression for the throughput metrics. Their work was extended to MIMO V-BLAST systems by Dekorsy [3] based on the conditional cut-off rate of MIMO transmission.

One of the features of the LTE technology is an ability of the eNodeB to adjust the Modulation and Coding Scheme (MCS) to the instantaneous channel conditions based on the Channel State Information (CSI). Szczecinski investigated the benefits of adaptive HARQ-IR, when the Modulation and Coding Scheme (MCS) changes over the retransmission rounds [4]. His simulations show that the adaptive HARQ brings significant gains compared to non-adaptive scheme for high SNR in channels with outdated CSI at the transmitter. The interesting results of the combination of HARQ and adaptive modulation and coding were obtained in [5], where with only one bit of feedback, the authors achieve performance close to the ergodic capacity. In this paper we strictly follow the 3GPP LTE standards [6], [7], [8], which define downlink HARQ protocol as non-adaptive and asynchronous.

The advanced MIMO receiver architecture takes cross-layer interference into account. This may put specific constrains on the design of the retransmission scheme [9]. Symbol-level combining scheme for HARQ with Interference-Aware (IA) successive decoding was proposed in [10]. The detailed analysis of the optimal combining schemes for MIMO systems with HARQ was done in [11]. In this paper we study the Single-User (SU) MIMO system with our Maximum-Likelihood (ML) IA Successive Interference Canceling (SIC) receiver [12] with HARQ protocol. The receiver passes the full received signal through the Matched Filter (MF) detector, computes IA soft LLR metric [13] for the first stream and decodes the first CW. After the first CW is successfully decoded, the receiver reconstructs it with the corresponding RV for a current and previous (if available) HARQ rounds, multiplies the signal with the corresponding compensated effective chan-

nel coefficients and subtracts it from the MF outputs so that the detection of the second stream is interference-free, thus benefiting from multi-round SIC LLRs combining for the second transport block (TB).

The majority of the state-of-art literature focuses on the methods to handle HARQ protocol in MIMO systems at the UE side. At the same time, there are very few sources describing the retransmission options of the eNodeB. In June 2016 we performed a drive test campaign in Sophia Antipolis, France, during which the full message flow between the eNodeB and the UE was captured. This allowed us to study the HARQ implementation in the practical MIMO LTE system with Ericsson eNodeB, configured in Cyclic Delay Diversity (TM3) using the DCI format 2A with 2 antenna ports. When the UE awaits to receive two TBs per subframe, they are associated with the same HARQ process. If only one CW is in error, the eNodeB performs a retransmission only of the erroneous CW, deactivating the CW that was successfully decoded. However, there is no precoding information field for the 2 antenna port configuration in the DCI format 2A. The transmit diversity (Alamouti precoding) is the only option available for the eNodeB for a retransmission of a single CW in TM3. This inspired us to study the retransmission strategies for Closed Loop Spatial Multiplexing (TM4) based on OpenAirInterface (OAI) [14] downlink (DL) simulator. TM4 uses the DCI format 2 with an active precoding information field for 2 antenna port transmission. For the single CW retransmission, the eNodeB uses Temporary Precoder Matrix Indicator (TPMI) in the DCI format 2 to signal the retransmission scheme.

Our main contributions in this paper are the following:

- We implement HARQ protocol support for the R-ML IA SIC receiver in OAI DL simulator.
- We perform the throughput and reliability analysis of TM4 with HARQ protocol with R-ML IA SIC and R-ML PIA receiver.
- We analyze different retransmission options applying the throughput metric in the situations with actual and outdated CSI in frequency-selective fading channels in the scenarios, when one of the CW is decoded, and another one is in error.

II. System Model

In this paper we often refer to the terms CW, TB and DCI. The MAC layer handles the TBs. The PHY layer maps TBs on the CWs. TB size defines a maximum number of bits that can be sent in 1 ms. The DCI can be seen as an interface between the MAC and PHY layers and carries the information about the MCS, New Data Indicator (NDI), RV, TPMI and resource allocation.

We consider 2×2 MIMO system, where the connection between the eNodeB and the UE is established in TM4 with DCI format 2 and 4 rounds HARQ-IR retransmission protocol is configured. The eNodeB sends TB^0 and TB^1 mapped onto spatially multiplexed CW^0 and CW^1 at the initial transmission round $r = 0$. The received signal vector $\mathbf{y}_l \in \mathbf{C}^{2\times 1}$ for the l-th subcarrier seen by the UE is given by

Table I: TPMI bit field interpretation for two CW transmission

Bit field	TPMI interpretation
0	$\frac{1}{2}\begin{bmatrix}1 & 1\\ 1 & -1\end{bmatrix}$
1	$\frac{1}{2}\begin{bmatrix}1 & 1\\ j & -j\end{bmatrix}$
2	last PMI on PUSCH

$$r = 0 : \mathbf{y}_l = \mathbf{H}_l \mathbf{P}_l \mathbf{x}_l + \mathbf{n}_l, \quad l = 1, 2..., L, \tag{1}$$

where $\mathbf{x}_l \in Q^{M_0,M_1}$ is the vector of two complex symbols x_0 and x_1 with variance of σ_0^2 and σ_1^2, $Q^{M_0,M_1} := Q^{M_0} \times Q^{M_1}$ is a Cartesian product of two modulation alphabets Q^{M_0} and Q^{M_1}, $M_0, M_1 \in \{2, 4, 6\}$ are the modulation orders of the QAM constellations. The vector $\mathbf{n}_l$ is Zero Mean Circularly Symmetric Complex Gaussian (ZMCSCG) white noise of double-sided power spectral density $N_0/2$ at the 2 receive antennas of UE. The matrix $\mathbf{H}_l$ is a 2×2 channel matrix built with respect to the applied in simulation section channel model and $\mathbf{P}_l$ is precoding matrix employed by the eNodeB at the l-th RE.

For the sake of simplicity, we drop the subcarrier index and replace the multiplication of $\mathbf{H}$ and $\mathbf{P}$ with the effective channel $\mathbf{H}_{\text{eff}}$:

$$\mathbf{y} = \mathbf{H}_{\text{eff}}\mathbf{x} + \mathbf{n}, \quad \mathbf{H}_{\text{eff}} = [\mathbf{h}_{\text{eff0}}\ \mathbf{h}_{\text{eff1}}]. \tag{2}$$

There are three precoding options signaled through the TPMI field for the DCI format 2 with 2 active CWs. The bit field to PMI interpretation is presented in Table I [8]. In our simulations, the eNodeB is configured to use TPMI2 — the PMI received with latest CSI report on Physical Uplink Shared Channel (PUSCH). Since with our SIC receiver decoding of CW^1 is only accessible if CW^0 is decoded correctly, the precoder is selected in the way to minimize the Block Error Rate (BLER) of the first stream. Specifically, the UE selects the precoder matrix $\mathbf{P}$, which ensures that the effective channel of the first stream is stronger than the one of the second stream by evaluating the correlation coefficient $\rho_{10} = \mathbf{h}_{\text{eff1}}^H\ \mathbf{h}_{\text{eff0}}$. Comparing the real and imaginary parts of ρ_{10}, the UE picks up one $\mathbf{P}$ from the two options:

$$\mathbf{P} = \begin{cases} \frac{1}{2}\begin{bmatrix}1 & 1\\ 1 & -1\end{bmatrix}, & \text{for } \Re(\rho_{10}) \geq \Im(\rho_{10}) \\ \frac{1}{2}\begin{bmatrix}1 & 1\\ j & -j\end{bmatrix}, & \text{for } \Re(\rho_{10}) < \Im(\rho_{10}) \end{cases} \tag{3}$$

III. R-ML IA SIC Receiver Implementation

Fig. 1 presents the basic scheme of R-ML IA SIC receiver. The received signal $\mathbf{y}$ (2) goes through the linear MF $\widehat{\mathbf{H}}_{\text{eff}}^H$. The received signal is transformed into

$$\begin{bmatrix} y_{MF_0} \\ y_{MF_1} \end{bmatrix} = \widehat{\mathbf{H}}_{\text{eff}}^H \mathbf{H} \begin{bmatrix} x_0 \\ x_1 \end{bmatrix} + \begin{bmatrix} n_0' \\ n_1' \end{bmatrix}, \tag{4}$$

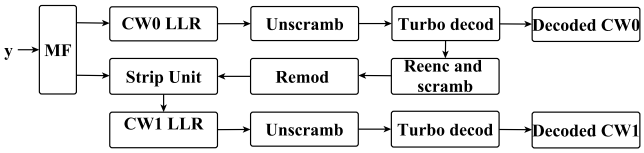

Figure 1: R-ML IA SIC receiver scheme

where $\widehat{\mathbf{H}}_{\text{eff}}$ is the estimated channel matrix.

The compensated signal belonging to the TB^1 is

$$y_{MF_1} = \left(\rho^* x_0 + \left(\widehat{h_{\text{eff01}}}^* h_{\text{eff01}} + \widehat{h_{\text{eff11}}}^* h_{\text{eff11}}\right) x_1\right) + n_1', \quad (5)$$

where $\rho^* = \widehat{h_{\text{eff01}}}^* h_{\text{eff00}} + \widehat{h_{\text{eff11}}}^* h_{\text{eff10}}$ is the correlation coefficient. After the MF, the receiver computes the IA soft bit LLR metric for lower-rate TB^0, treating TB^1 as interference. The bit metric for TB^0 is then passed to the turbo-decoder. If the Cyclic Redundancy Check (CRC) test confirms the correct decoding of TB^0, the SIC procedure is triggered. If the CRC fails, the LLR values of undecoded CWs are stored at the receiver and are updated during the next HARQ rounds.

The SIC block aims to reconstruct the decoded signal from the bits, belonging to TB^0. It performs re-encoding and re-modulation processes, multiplication of the symbols with the channel estimates, subtraction of the recovered signal from the MF output and LLR computation for TB^1.

After the stripping unit, TB^1 enjoys interference-free detection.

IV. Retransmission Protocols

Suppose TB^0 is decoded on the round $r = r_{dec}$. For all the rounds $r \leq r_{dec}$, the eNodeB sends a new RV of TB^0 and TB^1 that are mapped into CW^0 and CW^1 and stores the compensated received signal as well as the correlation coefficients.

$$r \leq r_{dec} : \text{TB}^0 \longmapsto \text{CW}^0, \text{TB}^1 \longmapsto \text{CW}^1.$$

The received signal vector is

$$\mathbf{y}_{\text{MF}r} = \widehat{\mathbf{H}}_{\text{eff}_r}^H \mathbf{H}_r \mathbf{x}_r + \mathbf{n}'_r, \quad r = 0, 1..., r_{dec}. \quad (6)$$

A. Multi-round SIC procedure

As soon as TB^0 is decoded, the multi-round SIC procedure is triggered. Since the UE now knows x_0, it may go through all the previous rounds $r = 0, 1..., r_{dec}$ to reconstruct $\rho_r^* x_{0r}$ with the corresponding RV, pass it through the stripping unit to obtain

$$\widetilde{y}_{\text{MF}_1 r} = \left(\widehat{h_{\text{eff01}r}}^* h_{\text{eff01}r} + \widehat{h_{\text{eff11}r}}^* h_{\text{eff11}r}\right) x_{1r} + n'_{1r} \quad (7)$$

and compute the corresponding multi-round interference-free LLR$_r^1$ metrics. After rate matching, that combines the multi-round LLRs, the receiver will make an attempt to decode TB^1. If the decoding is successful, the UE sends $\{\text{ACK}^0, \text{ACK}^1\}$ message to the eNodeB and moves to the next package. Otherwise, $\{\text{ACK}^0, \text{NACK}^1\}$ is sent, and if the limit of retransmission rounds has not been reached yet, the eNodeB will retransmit a new RV of TB^1.

Table II: TPMI bit field interpretation for a single CW retransmission

Bit field	TPMI interpretation
0	Alamouti
1	$\frac{1}{\sqrt{2}}\begin{bmatrix}1\\1\end{bmatrix}$
2	$\frac{1}{\sqrt{2}}\begin{bmatrix}1\\-1\end{bmatrix}$
3	$\frac{1}{\sqrt{2}}\begin{bmatrix}1\\j\end{bmatrix}$
4	$\frac{1}{\sqrt{2}}\begin{bmatrix}1\\-j\end{bmatrix}$
5	1st column of the last PMI on PUSCH
6	2nd column of the last PMI on PUSCH

B. Retransmission of TB^1

If TB^1 is not decoded after r_{dec} rounds of SIC procedure, it is not feasible to retransmit TB^0 again, thus, the eNodeB will deactivate it in the retransmission. The deactivation is performed through the DCI: the MCS for the deactivated TB is set to zero, while the corresponding RV is set to 1. If only one TB is active, it must be mapped on CW^0 [8]:

$$r_{dec} < r \leq (r_{max} - 1) : \text{TB}^1 \longmapsto \text{CW}^0, \text{TB}^0 \text{is disabled.}$$

After disabling TB^0, the eNodeB keeps DCI format 2 and faces a choice of the precoding options, which are signaled to the UE in TPMI. It includes Alamouti precoding and single layer precoding using either a predefined precoder or the one from latest CSI report on PUSCH. A TPMI bit field interpretation for the DCI format 2 for 2 antenna ports with one active CW is shown in Table II [8]. In this paper we focus on 3 options: TPMI $\in \{0, 5, 6\}$, since Alamouti precoding is designed to increase the reliability in low SNR regime, and TPMI5 and TPMI6 may improve system performance at high SNR.

Apart from the different TPMI options, we also consider two possibilities: if there is an actual CSI for each retransmission round r, or if the last CSI was received on r_{dec} and thus is outdated for the $r_{dec} < r \leq (r_{max} - 1)$ rounds when single TB^1 is retransmitted. Our precoder is optimal for CW^0, thus when TB^1 is mapped to CW^0, TPMI5 is expected to perform better than TPMI6. This makes the comparison between TPMI5 with actual CSI (assuming only PMI feedback, Channel Quality Indicator (CQI) is not taken into account) and TPMI6 with outdated CSI interesting.

a) TPMI0: The eNodeB configures the retransmission in Alamouti mode. In this case the received signal for rounds $r_{dec} < r \leq (r_{max} - 1)$ can be seen as:

$$\mathbf{y} = \frac{1}{\sqrt{2}}\mathbf{X}\mathbf{h} + \mathbf{n}, \quad (8)$$

where $\mathbf{X} = \begin{bmatrix} x_0 & x_1 \\ -x_1^* & x_0^* \end{bmatrix}$.

b) TPMI5 and TPMI6: the eNodeB configures the single layer retransmission based on the latest PMI report on PUSCH,

using precoder $\mathbf{p}$ from the first (TPMI5) or second (TPMI6) column multiplied by $\sqrt{2}$ of latest reported PMI. In this case the received signal for rounds $r_{dec} < r \leq (r_{max} - 1)$ can be seen as:

$$\mathbf{y} = \mathbf{H}\mathbf{p}x + \mathbf{n}. \tag{9}$$

The protocol implementation is described in Algorithm 1-Algorithm 3.

Algorithm 1 Retransmission algorithm for TM4 SIC detection

$r \leftarrow 0$, TPMI $\leftarrow 2$, $r_{max} \leftarrow 4$, $r_{sic} \leftarrow 0$
$\text{TB}^0_{flag} \leftarrow active$, $\text{TB}^0 \longmapsto \text{CW}^0$, $\text{TB}^1 \longmapsto \text{CW}^1$
$\text{TB}^0_{dec} \leftarrow false$, $\text{TB}^1_{dec} \leftarrow false$
while $(r \leq (r_{max} - 1))$ & $(\text{TB}^0_{dec} = false)$ **do**
    [eNodeB]: encoding, rate matching, modulation for both TBs.
    [UE]:measurements, feedback reporting on PUSCH.
    [UE]:MF and store the compensated channels.
    [UE]:LLR^0 computation and TB^0 decoding
    if TB^0 is decoded **then**
        $r = r_{dec}$
        $\text{TB}^0_{dec} = true$
        [UE]: call **procedure SIC**
    else
        [UE]: $\{\text{NACK}^0, \text{NACK}^1\}$
        $r \leftarrow r + 1$
    end if
end while

Algorithm 2 Multi-round SIC Procedure

procedure SIC(r_{dec}, MF outputs from previous rounds)
    for $0 \leq r_{sic} \leq r_{dec}$ **do**
        reconstruct $\rho^*_r x_{0r}$, obtain $y_{\text{MF},r_{sic}}$
        $LLR^1_{r_{sic}}$ computation
    end for
    Combine LLR^1 and decode TB^1
    if TB^1 is decoded **then**
        $\text{TB}^1_{dec} = true$, [UE]: ACK^0, ACK^1
        break ▷ Move to the next package
    else
        [UE]: $\{\text{ACK}^0, \text{NACK}^1\}$
        $r \leftarrow r + 1$
        [UE]: call **procedure Retransmit TB**^{1}
    end if
end procedure

Algorithm 3 Retransmit TB^1

procedure Retransmit TB$^1(r)$
    $\text{TB}^0_{flag} \leftarrow deactivated$, $\text{TB}^1 \longmapsto \text{CW}^0$
    [eNodeB]: choose TPMI $\in \{0, 1..6\}$
    for $r \leq (r_{max} - 1)$ **do**
        [eNodeB]: encoding, rate matching, modulation for TB^1.
        [UE]:MF and store the compensated channels.
        [UE]:LLR^1 computation and combining
        [UE]:TB^1 decoding
        if TB^1 is decoded **then**
            $\text{TB}^1_{dec} = true$, [UE]: $\{\text{ACK}^0, \text{ACK}^1\}$
            break ▷ Move to the next package
        else
            [UE]: $\{\text{ACK}^0, \text{NACK}^1\}$
            $r \leftarrow r + 1$
        end if
    end for
end procedure

V. Numerical Results and Discussion

A. Simulation parameters

The link-level simulations (LLS) were carried out for the 5 MHz 8-tap Rayleigh fading channel and Extended Pedestrian A (EPA) channel [15] with zero Doppler frequency. For the EPA channel modeling we applied low and moderate correlation matrix, referring to them as to EPAL and EPAM respectively. The eNodeB sends 3000 packets with 1 Physical Downlink Control Channel symbol over the wide range of noise variances. Every retransmission round is drawn from a new channel realization. Since TM4 is designed for high data rates transmission, we chose MCS^0 and MCS^1, such that $10 \leq \text{MCS}^0 \leq 28$, $\text{MCS}^0 \leq \text{MCS}^1 \leq 28$. For each fading environment we consider three retransmission options: TPMI0, TPMI5 with actual CSI, and TPMI6 with outdated CSI.

B. MCS Optimization and Throughput Analysis for the Multiple Rounds

The total system throughput of the MIMO system with 2 TBs and $r_{\max}$ HARQ rounds can be seen as

$$T_{\text{tot}} = \sum_{r=0}^{r_{\max}-1} (T^0_r + T^1_r), \tag{10}$$

$$T^0_r = \frac{1}{r+1} R^0 (1 - BLER^0_r), \quad T^1_r = \frac{1}{r+1} R^1 (1 - BLER^1_r),$$

where T^0_r and T^1_r are the throughput values for TB^0 and TB^1 on the round r, R^0 and R^1 are the rates corresponding to MCS^0 and MCS^1, $BLER^0_r$ and $BLER^1_r$ are the corresponding Block Error Rates. The fact that CW^1 is attempted for a decoding only if CW^0 is decoded is taken into account in BLER.

SIC receivers are very sensitive to the choice of MCS: if the instantaneous channel does not support the rate of MCS^0, CW^0 is not decoded and the SIC procedure is thus not triggered. On the other hand, if the first stream is decoded, the second stream becomes interference-free and can potentially carry higher information rates. There exist an optimal combination of $\text{MCS}^{\star 0}$ and $\text{MCS}^{\star 1}$ that maximizes averaged long-term throughput (10). We apply the methodology from [12]: LLS traces are generated for all possible MCS combinations for 4 HARQ rounds. After that for each SNR point we select $\text{MCS}^{\star 0}$ and $\text{MCS}^{\star 1}$, which corresponds to the maximum throughput.

Spectral efficiency declines with every retransmission round due to reuse of space-frequency resources by the same TB. Thus, the maximum contribution to the averaged long-term throughput is done during the first round. In the previous publication [12], that was recently submitted, we showed that our SIC receiver achieves up to 1.8 Mbps throughput gain in 5 MHz bandwidth flat Rayleigh fading compared to our R-ML IA receiver [16] in scenarios without HARQ protocol. In this paper we extend the comparison to the multiple HARQ rounds and frequency-selective Rayleigh 8-tap and EPA channel models. Fig. 2 illustrates the total system throughput T_{tot} after 4 HARQ rounds and throughput $T^0_0 + T^1_0$

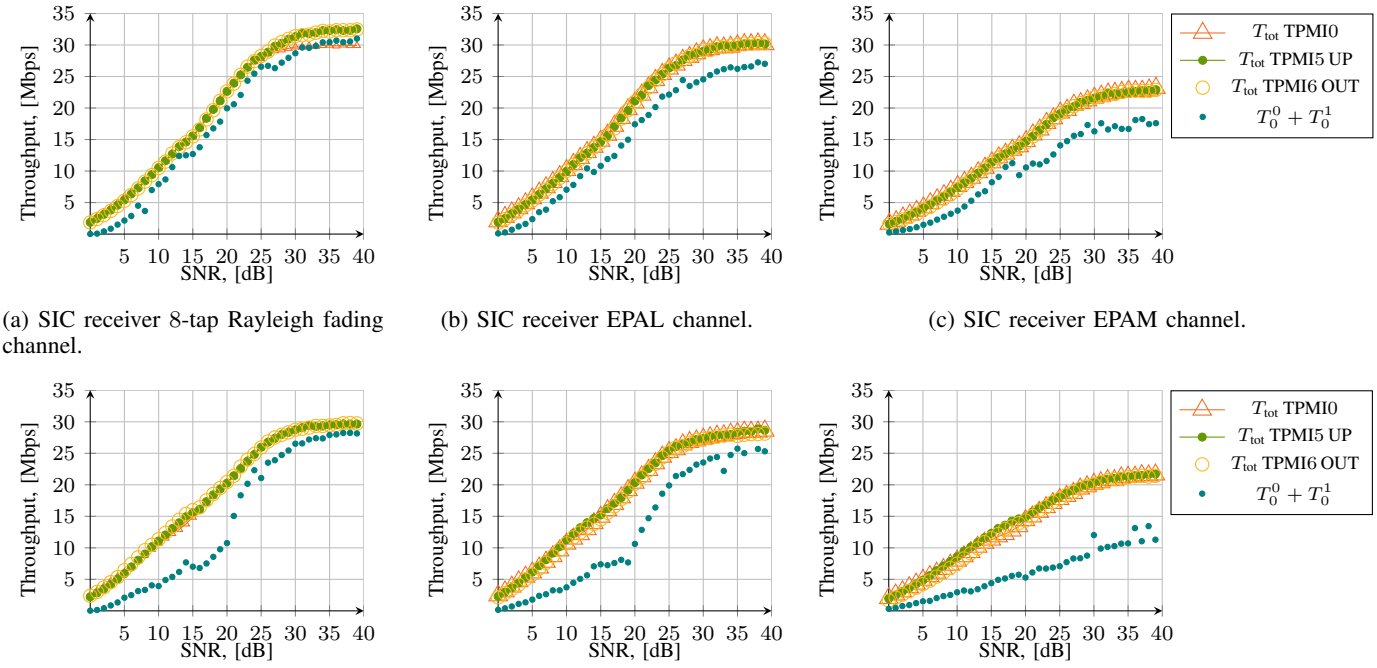

(a) SIC receiver 8-tap Rayleigh fading channel.

(b) SIC receiver EPAL channel.

(c) SIC receiver EPAM channel.

(d) PIA receiver 8-tap Rayleigh fading channel.

(e) PIA receiver EPAL channel.

(f) PIA receiver EPAM channel.

Figure 2: Comparison of SIC and PIA receiver's total throughput T_{tot} after 4 HARQ rounds and throughput $T_0^0 + T_0^1$ after the first round $r = 0$ applying optimized MCS$^{\star 0}$ and MCS$^{\star 1}$. We consider TPMI=$\{0, 5, 6\}$ during the retransmissions of single TB^1. TPMI5 is studied in updated CSI scenario, while TPMI6 is considered in outdated CSI environment. Throughput $T_0^0 + T_0^1$ after the first round is independent from the TPMI used during the retransmissions of single TB^1.

after the first round $r = 0$ achieved with MCS$^{\star 0}$ and MCS$^{\star 1}$ for SIC and PIA detection. Our SIC receiver outperforms the PIA receiver on the first round $r = 0$ in all the channel models with the gains varying from $2 - 4$ Mbps in high SNR regime to $5 - 7$ Mbps in low SNR regime. Multiple retransmission rounds reduce this gap, but the SIC receiver still performs better at high SNR (up to $2 - 3$ Mbps). The worse the channel is, the bigger is the contribution of the retransmissions in terms of throughput. However, the TPMI during single TB retransmission does not have a noticeable impact on the throughput. There is a slight preference to TPMI5 and TPMI6 in actual and outdated CSI scenarios over Alamouti coding in the frequency-selective Rayleigh channel, while in EPA channels there is no visible difference.

C. Reliability Analysis

In this section we focus on the contribution of the multiple HARQ rounds to the reliability of the MIMO system with our SIC receiver. The MCS optimization methodology applied in the previous section fits well to provide an initial idea about throughput, achievable with multiple HARQ rounds. However, it reflects poorly the TPMI influence on the system performance in the cases with a single CW retransmission. For the following reliability analysis we detach from the optimized MCS$^{\star 0}$ and MCS$^{\star 1}$ and consider a few particular MCS. To cover all the modulation orders, we select three MCS combinations: MCS$^0 = 12$ and MCS$^1 = 16$, MCS$^0 = 16$ and MCS$^1 = 20$, MCS$^0 = 20$ and MCS$^1 = 26$.

The main contribution from the HARQ protocol is performance improvement in the lower SNR regime. Fig. 3 introduces the BLER of TB^0 for 4 HARQ rounds. At the target BLER level of 10^{-1}, the $12 - 16$ MCS combination receives 10 dB and 13.5 dB improvement in Rayleigh and EPA channel respectively. The SNR gain increases for the higher MCS and reaches 12 and 20 dB for $16 - 22$ and $22 - 26$ MCS combinations in Rayleigh and EPAM channel respectively. However, these benefits are coming at price of spectral efficiency degradation with every retransmission round, as the space-frequency resources are reused by the same TB. Since the first stream is treated by the SIC and PIA receivers in the same way, the R-ML PIA receiver is expected to show identical performance for TB^0.

We illustrate the analysis of the second stream with examples from the EPAM channel, in which there is a significant ($\approx$ 5Mbps) difference in throughput performance between scenarios with 4 HARQ rounds and scenarios without HARQ, as we previously showed on Fig. 2.

After TB^0 is decoded on round r_{dec}, the SIC receiver reconstructs TB^0 with the corresponding RV for each round $0 \leq r \leq r_{dec}$, thus obtaining multi-round LLRs for TB^1. Fig. 4 shows, how many frames belonging to TB^1 were passed to the multi-round SIC procedure and how many were suc-

cessfully decoded through it on the round r. In the low SNR regime, a negligible amount of attempts was done at $r = 0$ due to the high BLER of TB^0 in Fig. 3, while a significant amount of them was performed in the next rounds, since the BLER of TB^0 is remarkably lower after retransmissions even at low SNR. However, the majority of attempts failed, meaning that the gain from the LLR combining through multi-round SIC procedure is not sufficiently high to improve the performance in the low SNR regime. At moderate SNR level, about 50% of the attempts are decoded through the SIC procedure, while in high SNR level this value reaches 100%. We conclude that our SIC receiver implementation benefits from multi-round LLR combining at moderate SNR and the majority of combining gain is coming from the second round $r = 1$, while in the low SNR regime gains are not that impressive.

At each round $(r > 0)$, the total amount of retransmissions ret_r^{tot} is composed from the fraction of single TB retransmissions ret_r^{single} and the fraction of two TBs retransmission ret_r^{multipl}:

$$ret_r^{\text{single}} = ret_r^{\text{tot}} - ret_r^{\text{multipl}}. \quad (11)$$

In Fig. 5 we compare the amount of retransmissions of single TB^1 ret_r^{single} on round r in EPAM channel for our SIC and PIA receivers. In the low SNR regime the amount of ret_r^{single} is almost identical, while in moderate and high SNR regime SIC receiver has about 50% less of ret_r^{single} due to the benefits of LLR combining through multi-round TB^0 reconstruction and subsequent subtraction. This supports the idea that the main benefits of SIC receiver are achieved during the first two rounds $r = 0$ and $r = 1$. In practice, there are cases for the PIA receiver, when TB^1 is decoded, while TB^0 is in error. In this case TB^1 is deactivated and the UE requests the retransmission of single TB^0. Such cases are negligibly rare due to our precoder selection strategy, that maximizes the probability of CW^0 to be decoded.

We now investigate the BLER of TB^1(Fig. 6). At the very first round $r = 0$ with all the MCS combinations, our SIC receiver significantly outperforms PIA detection due to the SIC procedure, for example, it achieves BLER of 10^{-1} at SNR level 10 dB lower than for PIA receiver for $12 - 16$MCS combination. The SNR level for BLER of 10^{-1} is slightly lower for the SIC receiver after the first round, while the following retransmission rounds are bringing significant benefits to the PIA detection, while for the SIC receiver gain between the third and fourth retransmission round is not remarkable.

Regarding the TPMI for the ret_r^{single}, both receivers show slight preference for the Alamouti precoding. This means, that the retransmission scheme, employed by the Ericsson eNodeB for TM3 is the optimal retransmission scheme for TM4.

D. A Note on Computational Effort

In the preceding work [12] we showed, that our SIC receiver is 25% more time efficient than our PIA receiver given only one transmission round. However, there are less retransmissions of the single TB^1 in high SNR regime with HARQ support if SIC detection is applied, meaning that overall processing time is further reduced. On the other side, the SIC detection clearly has high CPU consumption, since we need to store the MF outputs and correlation coefficients for TB^0 for each retransmission to be able to reconstruct the signal from preceding rounds.

VI. Conclusion

Inspired by the drive test measurement campaign, we have presented HARQ protocol implementation for our R-ML IA SIC and R-ML PIA receivers for LTE TM4 in OAI DL simulator. The SIC receiver achieves higher throughput in all the simulated scenarios. For both receivers, the first TB accesses huge performance improvement in the low SNR regime thanks to HARQ (up to 10 dB reduction to achieve BLER of 10^{-1}) at the price of spectral efficiency degradation with every retransmission round, as the space-frequency resources are reused by the same TB. The Ericsson eNodeB that was used to perform the drive tests, was configured in TM3 and applied Alamouti precoding as the only option allowed by the DCI for this transmission mode. Our analysis for the DCI format 2 showed that Alamouti precoding is favorable for the retransmissions of the single CW in TM4 from the reliability point of view, while there is no noticeable preference to any of the retransmission schemes from the throughput point of view.

The future publication will provide the feedback computation methodology for PIA and SIC receivers and extend our analysis to TM3.

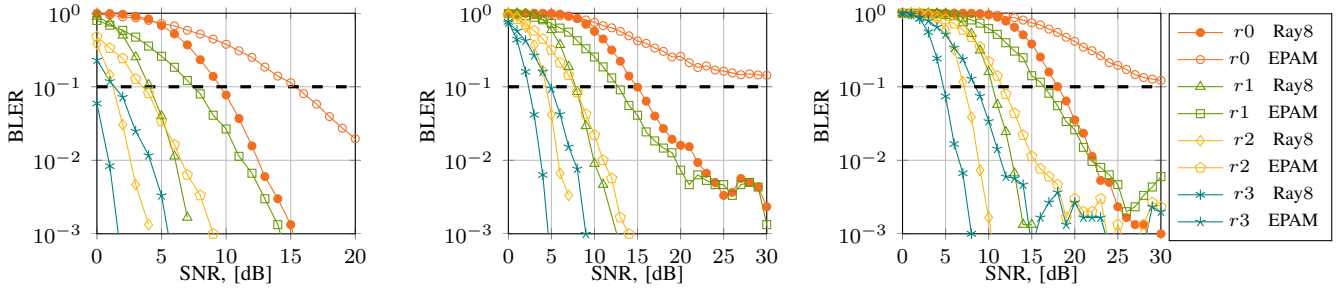

(a) MCS^0 = 12, MCS^1 = 16. (b) MCS^0 = 16, MCS^1 = 22. (c) MCS^0 = 20, MCS^1 = 26.

Figure 3: BLER of TB^0 in 8-tap Rayleigh and EPAM channels for 4 HARQ rounds (identical for SIC and PIA receiver).

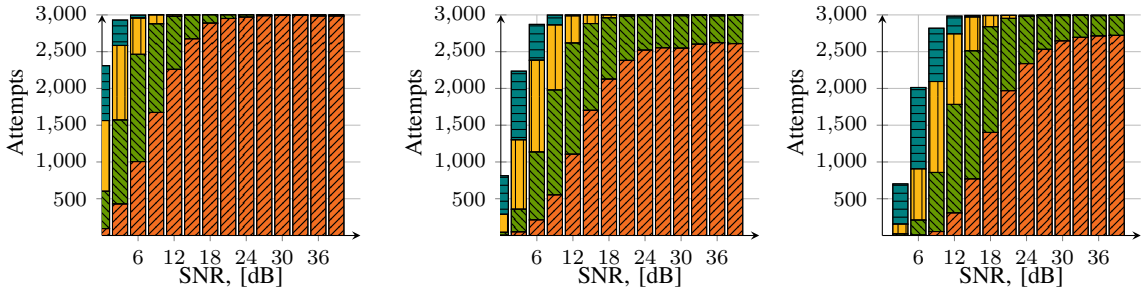

(a) $\text{MCS}^0 = 12$, $\text{MCS}^1 = 16$.

(b) $\text{MCS}^0 = 16$, $\text{MCS}^1 = 22$.

(c) $\text{MCS}^0 = 20$, $\text{MCS}^1 = 26$.

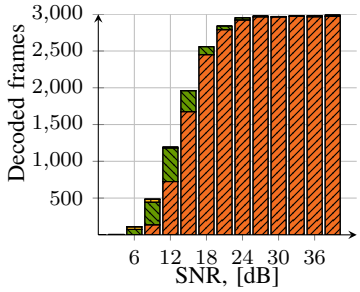

(d) $\text{MCS}^0 = 12$, $\text{MCS}^1 = 16$.

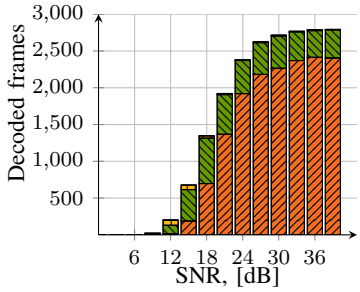

(e) $\text{MCS}^0 = 16$, $\text{MCS}^1 = 22$.

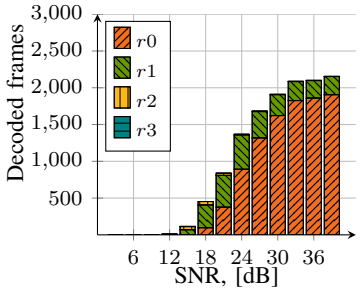

(f) $\text{MCS}^0 = 20$, $\text{MCS}^1 = 26$.

Figure 4: Amount of TB^1 frames attempted to be decoded (a,b,c) and successfully decoded (d,e,f) through SIC procedure for the round r in EPAM channel.

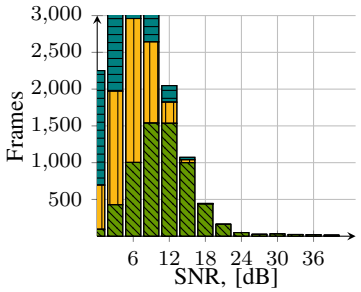

(a) $\text{MCS}^0 = 12$, $\text{MCS}^1 = 16$, SIC receiver.

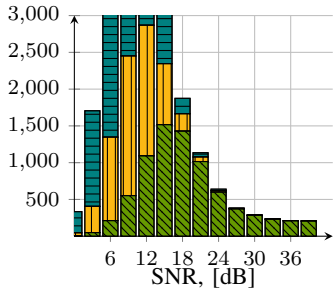

(b) $\text{MCS}^0 = 16$, $\text{MCS}^1 = 22$, SIC receiver.

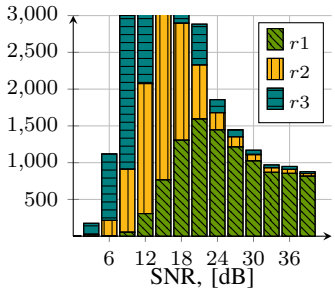

(c) $\text{MCS}^0 = 20$, $\text{MCS}^1 = 26$, SIC receiver.

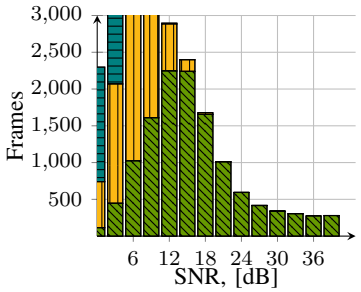

(d) $\text{MCS}^0 = 12$, $\text{MCS}^1 = 16$, PIA receiver.

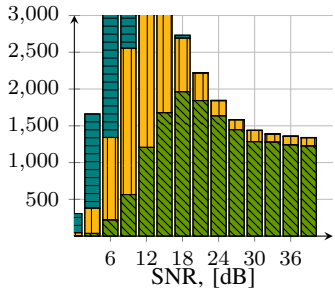

(e) $\text{MCS}^0 = 16$, $\text{MCS}^1 = 22$, PIA receiver.

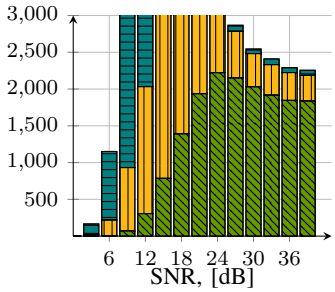

(f) $\text{MCS}^0 = 20$, $\text{MCS}^1 = 26$, PIA receiver.

Figure 5: Amount of retransmissions of single TB^1 ret_r^{single} on round r in EPAM channel for SIC (a,b,c) and PIA (d,e,f) receivers.

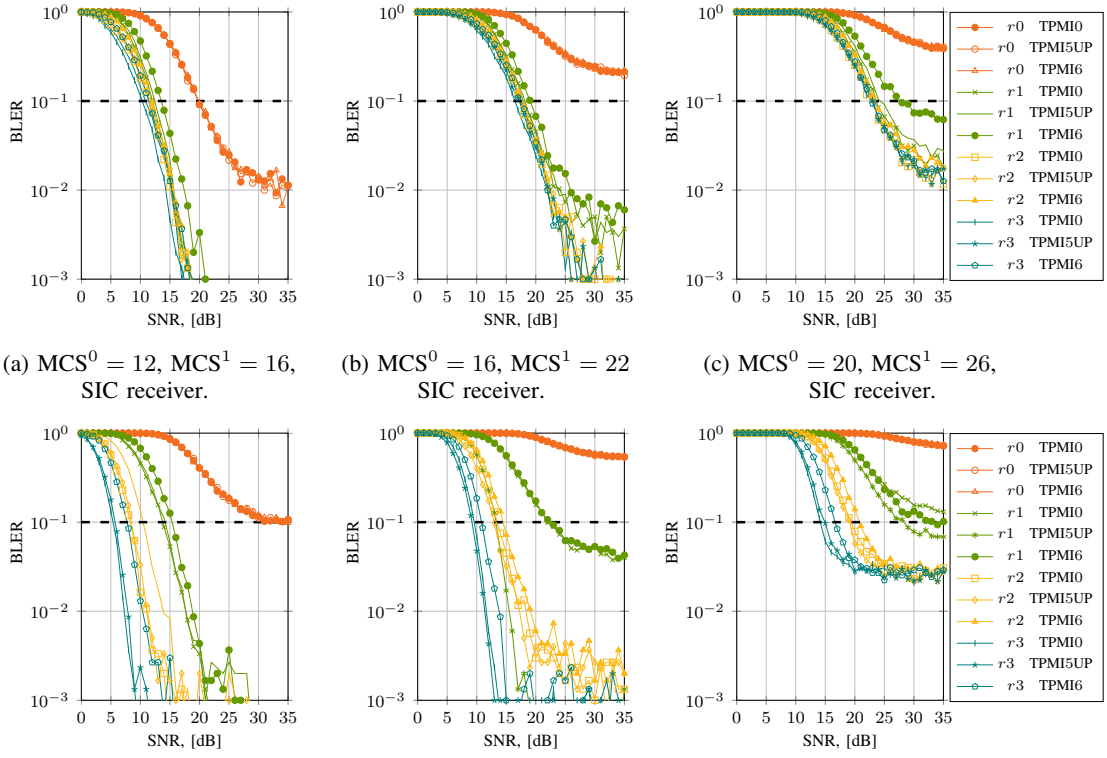

(a) $\text{MCS}^0 = 12$, $\text{MCS}^1 = 16$, SIC receiver.

(b) $\text{MCS}^0 = 16$, $\text{MCS}^1 = 22$ SIC receiver.

(c) $\text{MCS}^0 = 20$, $\text{MCS}^1 = 26$, SIC receiver.

(d) $\text{MCS}^0 = 12$, $\text{MCS}^1 = 16$, PIA receiver.

(e) $\text{MCS}^0 = 16$, $\text{MCS}^1 = 22$, PIA receiver.

(f) $\text{MCS}^0 = 20$, $\text{MCS}^1 = 26$, PIA receiver.

Figure 6: BLER of TB^1 in EPAM channel for 4 HARQ rounds for SIC (a,b,c) and PIA (d,e,f) receiver for TPMI=$\{0, 5, 6\}$. TPMI5 is studied in updated CSI scenario, while TPMI6 is considered in outdated CSI environment.

REFERENCES

[1] E. N. Onggosanusi, A. G. Dabak, Y. Hui, and G. Jeong, "Hybrid arq transmission and combining for mimo systems," in *Communications, 2003. ICC '03. IEEE International Conference on*, vol. 5, May 2003, pp. 3205–3209 vol.5.

[2] G. Caire and D. Tuninetti, "The throughput of hybrid-arq protocols for the gaussian collision channel," *IEEE Transactions on Information Theory*, vol. 47, no. 5, pp. 1971–1988, 2001.

[3] A. Dekorsy, "A cutoff rate based cross-layer metric for mimo-harq transmission," in *2005 IEEE 16th International Symposium on Personal, Indoor and Mobile Radio Communications*, vol. 4, Sept 2005, pp. 2166–2170 Vol. 4.

[4] L. Szczecinski, C. Correa, and L. Ahumada, "Variable-rate transmission for incremental redundancy hybrid arq," in *Global Telecommunications Conference (GLOBECOM 2010), 2010 IEEE*, Dec 2010, pp. 1–5.

[5] T. Villa, R. Merz, R. Knopp, and U. Takyar, "Adaptive modulation and coding with hybrid-arq for latency-constrained networks," in *European Wireless, 2012. EW. 18th European Wireless Conference*, April 2012, pp. 1–8.

[6] 3GPP, "Evolved universal terrestrial radio access (e-utra); physical layer procedures," 3GPP, Tech. Rep. Technical Specification 36.213–V12.3, Oct 2014.

[7] ——, "Evolved universal terrestrial radio access (e-utra); physical channels and modulation," 3GPP, Tech. Rep. Technical Specification 36.211–V12.6.0, July 2015.

[8] ——, "Evolved universal terrestrial radio access (e-utra); multiplexing and channel coding," 3GPP, Tech. Rep. Technical Specification 36.212–V12.7.0, July 2015.

[9] D. Toumpakaris, J. Lee, A. Matache, and H. L. Lou, "Performance of mimo harq under receiver complexity constraints," in *IEEE GLOBECOM 2008 - 2008 IEEE Global Telecommunications Conference*, Nov 2008, pp. 1–5.

[10] H. Kwon, J. Lee, and I. Kang, "Symbol-level combining for hybrid arq on interference-aware successive decoding," in *2013 IEEE Global Communications Conference (GLOBECOM)*, Dec 2013, pp. 3650–3654.

[11] E. W. Jang, J. Lee, H. L. Lou, and J. M. Cioffi, "Optimal combining schemes for mimo systems with hybrid arq," in *2007 IEEE International Symposium on Information Theory*, June 2007, pp. 2286–2290.

[12] E. Lukashova, F. Kaltenberger, and R. Knopp, "ML successive interference cancelling vs parallel interference aware detection in LTE SU-MIMO systems," in *Submitted to 2017 European Conference on Networks and Communications (EuCNC): Physical Layer and Fundamentals (PHY) (EuCNC2017 - PHY)*, Oulu, Finland, Jun. 2017.

[13] R. Ghaffar and R. Knopp, "Low complexity metrics for bicm siso and mimo systems," in *Vehicular Technology Conference (VTC 2010-Spring), 2010 IEEE 71st*, May 2010, pp. 1–6.

[14] OpenAirInterfacePlatform, Eurecom. [Online]. Available: http://www.openairinterface.org/

[15] 3GPP, "Evolved universal terrestrial radio access (e-utra); User Equipment (UE) radio transmission and reception," 3GPP, Tech. Rep. Technical Specification 36.101–V12.9.0, Oct 2015.

[16] E. Lukashova, F. Kaltenberger, R. Knopp, and C. Bonnet, "PHY layer abstraction for SU-MIMO LTE system employing parallel Interference-Aware detection," in *International Workshop on Link and System Level Simulations 2016 (IWSLS2'16)*, Vienna, Austria, June 2016.